

Title	Sonication-assisted supramolecular nanorods of meso-diaryl-substituted porphyrins
Author(s)	Hasobe, Taku; Oki, Hideaki; Sandanayaka, Atula S. D.; Murata, Hideyuki
Citation	Chemical Communications, 2008(6): 724-726
Issue Date	2008
Type	Journal Article
Text version	author
URL	<a href="http://hdl.handle.net/10119/7908">http://hdl.handle.net/10119/7908</a>
Rights	Copyright (C) 2008 Royal Society of Chemistry. Taku Hasobe, Hideaki Oki, Atula S. D. Sandanayaka and Hideyuki Murata, Chemical Communications, 2008(6), 2008, 724-726. <a href="http://dx.doi.org/10.1039/b713971c">http://dx.doi.org/10.1039/b713971c</a> - Reproduced by permission of The Royal Society of Chemistry
Description	

# Sonication-assisted supramolecular nanorods of *meso*-diaryl-substituted porphyrins

Taku Hasobe<sup>\*a,b</sup>, Hideaki Oki<sup>a</sup>, Atula S. D. Sandanayaka<sup>a</sup>, and Hideyuki Murata<sup>\*a</sup>

Received (in XXX, XXX) 1st January 2007, Accepted 1st January 2007

First published on the web 1st January 2007

DOI: 10.1039/b000000x

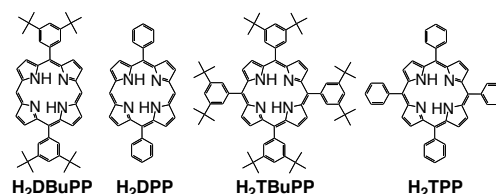
5 **Supramolecular nanorods of 5,15-diaryl substituted porphyrins prepared by sonication method exhibit a broad absorption property, which is confirmed by photocurrent generation measurement in a photoelectrochemical cell.**

Organized molecular assemblies with well-defined shapes and  
10 structures are of great interest because of a variety of applications (i.e., photonics, electronics, and solar energy conversion etc.).<sup>1,2</sup> Porphyrins are often organized into nanoscale superstructures which perform many of the essential light-harvesting and electron- and energy-transfer functions.<sup>3,4</sup> Most pursuits of  
15 porphyrin assemblies toward construction of the molecular architectures have been focused on the connection of porphyrin units with strong bonds such as covalent and coordination bonds,<sup>3,5</sup> since the intermolecular interactions such as  $\pi$ - $\pi$  stacking, van der Waals, and hydrophobic interactions are considered to be  
20 too weak to maintain the superstructures. Especially, construction of the anisotropic bar-shaped assemblies of porphyrins (i.e., rod- and tube-structures)<sup>6</sup> based on these 'weak' interactions becomes a further challenge as compared to the spherical-shaped assemblies.<sup>7</sup>

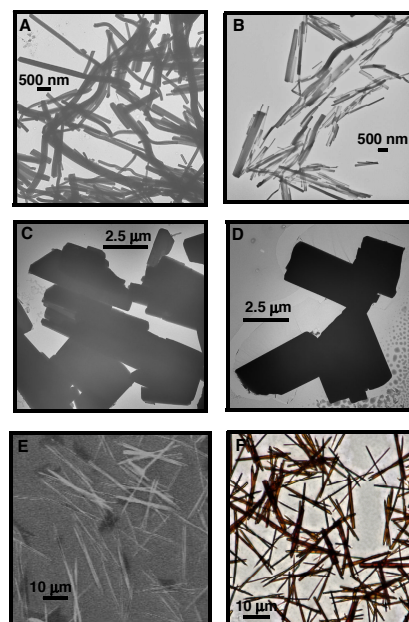
25 Ultrasonic wave is often utilized for formation of crystal nucleus and growth in the preparation of molecular crystals<sup>8</sup> but seldom favors the formation of an ordered assembly. We report herein novel supramolecular nanorods and fibers controlled by intermolecular interactions such as  $\pi$ - $\pi$  stacking interaction of  
30 porphyrins without the other bonds/interactions or aiding surfactants, which are prepared in sonicated solution medium. In this study, we employed 5,15-diaryl-substituted porphyrins (H<sub>2</sub>DBuPP and H<sub>2</sub>DPP) and the fully *meso*-substituted reference porphyrins: 5,10,15,20-tetraaryl-substituted porphyrins  
35 (H<sub>2</sub>TBuPP and H<sub>2</sub>TPP) to examine substituent effect on the assembled structures (Chart 1). Porphyrin-based supramolecular nanorods and fibers are successfully organized by proper configuration of substituents in a porphyrin plane and utilizing ultrasonic wave. Additionally, the organized structure exhibits an  
40 unusual broad photoresponse in the visible region, which is confirmed by absorption, excitation and photoelectrochemical action spectra.

The synthesis of H<sub>2</sub>DBuPP, H<sub>2</sub>TBuPP and H<sub>2</sub>DPP has been reported previously.<sup>9</sup> The porphyrin nanorod was prepared by the  
45 following procedure. First, 3.5 mmol dm<sup>-3</sup> porphyrin solution was prepared in toluene. Then, the toluene solution is simply mixed with 9 times volume of acetonitrile (final concentration: 0.35

mmol dm<sup>-3</sup> in a poor/good solvent = 9/1, v/v). The solution was sonicated (45 kHz) for 30 min at 15 °C to form macroscopic self-assembled porphyrins such as rod-like structures by using our original set-up (See: experimental section of supporting information). It should be noted that no formation of rod-like structure is observed without sonication,<sup>10</sup> and all measurements for analysis of the structures were performed quickly before  
50 occurrence of the precipitation. Fig. 1A and B shows TEM images of these self-assembled nanorods of H<sub>2</sub>DBuPP and H<sub>2</sub>DPP, respectively.



60 **Chart 1.** Porphyrin compounds bearing different substituents at *meso*-positions in this study.



65 **Fig. 1** TEM images of (A) H<sub>2</sub>DBuPP nanorod, (B) H<sub>2</sub>DPP nanorod, (C) H<sub>2</sub>TBuPP assembly, and (D) H<sub>2</sub>TPP assembly. SEM and optical microscope images of H<sub>2</sub>DBuPP fiber are (E) and (F), respectively.

<sup>a</sup>School of Materials Science, Japan Advanced Institute of Science and Technology, Nomi, Ishikawa, 923-1292, Japan. Fax: +81 761 51 1149; E-mail: t-hasobe@jaist.ac.jp, murata-h@jaist.ac.jp, <sup>b</sup>PRESTO, Japan Science and Technology Agency (JST), 4-1-8 Honcho, Kawaguchi, Saitama, Japan.

†Electronic Supplementary Information (ESI) available: Experimental part, length-distributions, SEM and optical microscope images, XRD measurement, fluorescence lifetime, MULDI/TOF MASS, crystal structure analysis. See DOI: 10.1039/b000000x/

In contrast with large square crystal structures (2-3  $\mu$ m scale) of the respective references: H<sub>2</sub>TBuPP and H<sub>2</sub>TPP assemblies (Fig. 1C and D), H<sub>2</sub>DBuPP and H<sub>2</sub>DPP assemblies form a lot of long

rod-structures (denoted as H<sub>2</sub>DBuPP or H<sub>2</sub>DPP nanorods). For example, the structure of H<sub>2</sub>DBuPP nanorods are 360 ± 130 nm in diameter and 5.02 ± 1.94 μm in length (Fig. S2).<sup>11</sup> In both of SEM and optical microscope images, the same structures are observed (Fig. S3).<sup>12</sup> Judging from molecular scale of a porphyrin, it is likely that H<sub>2</sub>DBuPP or H<sub>2</sub>DPP undergoes linear assembly to yield large rod-like structures. This indicates that substituents at *meso*-positions largely contribute to the control of intermolecular interaction between porphyrins for macroscopic organization.

The internal structures of the self-assembled porphyrins are investigated by XRD analysis (Fig. S5). Both of the peaks in XRD patterns (patterns *a*) of self-assembled porphyrins (H<sub>2</sub>DPP nanorod and H<sub>2</sub>TPP assembly) are consistent with the patterns of respective H<sub>2</sub>DPP and H<sub>2</sub>TPP bulk starting materials (patterns *b*), which confirms that the porphyrin assemblies consist of pristine H<sub>2</sub>DPP and H<sub>2</sub>TPP.<sup>13</sup> To further confirm the crystal structure and self-assembled aggregate mode, we have also theoretically simulated the XRD patterns as shown in patterns *c*.<sup>6e</sup> It can be found that the peaks in the XRD patterns of self-assembled H<sub>2</sub>DPP and H<sub>2</sub>TPP are assigned according to the simulated patterns from the corresponding crystal structures.<sup>14</sup> The strong two peaks [(100) and (002)] in H<sub>2</sub>DPP nanorod may show a particular orientation of porphyrin moieties.<sup>15</sup>

We have also succeeded in construction of much longer fiber structures by the following additional operations. The preparation method of nanorod assembly is the same as the above-mentioned one. The nanorod suspended solution is further allowed to stand for 6 days. Then, the crystallized porphyrins were stirred for 5 min at room temperature. The nanorod crystals finally grow up to be longer fiber structures (denoted as H<sub>2</sub>DBuPP fiber). The SEM and optical microscope images of H<sub>2</sub>DBuPP fibers are shown in Fig. 1E and F. In both images, we can clearly see much longer fiber structures analyzed as 890 ± 270 nm in diameter and 27.2 ± 6.9 μm in length (Fig. S2C). In the formation of the fiber structures, a large increase of length from 5.0 to 27.2 μm (~6 times) relative to that of diameter (~2 times) indicates that anisotropic crystal growth largely occurs toward the length direction. Thus, we have successfully controlled the structures of porphyrin fibrous assemblies within a certain definite range.<sup>16</sup>

We have also measured steady-state absorption and fluorescence spectra of H<sub>2</sub>DBuPP nanorods on a quartz plate as shown in Fig. 2A and B to examine electronic interaction of porphyrins in nanorod structures. In the measurement of absorption spectra, we employed an integrating sphere to avoid the scattering effect on the apparent absorption. The absorption spectrum of H<sub>2</sub>DBuPP nanorod exhibits much broader and more intense absorption in the visible and near infrared regions than those of the corresponding simple drop-cast film prepared by H<sub>2</sub>DBuPP in toluene (spectrum *b*) and toluene solution (spectrum *c*). This change of absorption property is likely because of strong supramolecular π-π interaction between a porphyrin and its nearest neighbor in nanorod structures.<sup>3a</sup> The broad absorption is also confirmed by the corresponding excitation spectrum and photoelectrochemical measurement (*vide infra*). Taking into consideration reversible structural change between the self-assembled structure and monomeric form<sup>13</sup> in addition to the broad absorption property, we can suppose that π-π interaction of porphyrin rings plays a significant role for the organization. Moreover, in fluorescence measurement of H<sub>2</sub>DBuPP nanorod (Fig. 2B and S9), the strong fluorescence quenching property is also observed by the lifetime analysis.<sup>17</sup> Since stable fluorescence

of H<sub>2</sub>DBuPP nanorod is observed, we have also measured fluorescence images of H<sub>2</sub>DBuPP nanorod and fiber. In both cases, uniform luminous structures were observed in Fig. 2C.

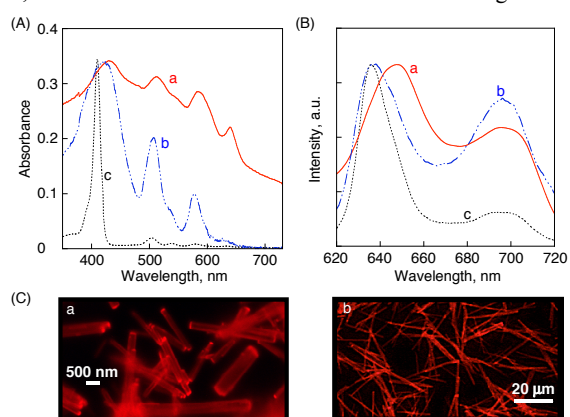


**Fig. 2** (A) Absorption and (B) fluorescence spectra of (a) H<sub>2</sub>DBuPP nanorod film, (b) H<sub>2</sub>DBuPP drop-cast film on quartz plates and (c) H<sub>2</sub>DBuPP (4 × 10<sup>-6</sup> mol dm<sup>-3</sup>) in toluene. The excitation wavelength is 410 nm. (C) Fluorescence images of (a) H<sub>2</sub>DBuPP nanorod and (b) H<sub>2</sub>DBuPP fiber.

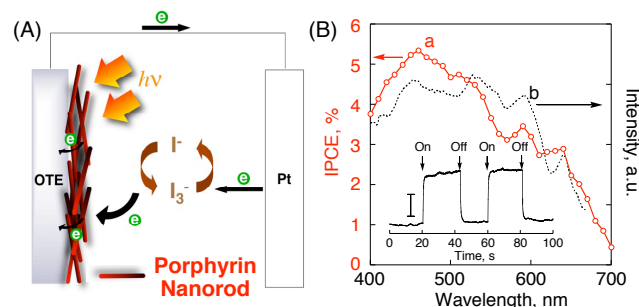


**Fig. 3** (A) An illustration of the photoelectrochemical solar cell. (B) (a) Photocurrent (IPCE) action spectrum of H<sub>2</sub>DBuPP nanorod on an OTE. Electrolyte: 0.5 mol dm<sup>-3</sup> LiI and 0.01 mol dm<sup>-3</sup> I<sub>2</sub> in acetonitrile. (b) Excitation spectrum of H<sub>2</sub>DBuPP nanorod on an OTE; Observed at 710 nm. The insertion shows photocurrent generation responses under white light illumination using an AM 1.5 filter. Input Power: 42 mW cm<sup>-2</sup>. The bar is 50 mA/cm<sup>2</sup>.

The spectroscopic behaviors in this organized fibrous structures are further promising for optical and electrical application, and we constructed a photoelectrochemical cell composed of H<sub>2</sub>DBuPP nanorod-modified optically transparent electrode (OTE) [denoted as OTE/H<sub>2</sub>DBuPP-n] by drop casting to examine the semiconducting behavior.<sup>4,18</sup> Fig. 3A shows an illustration of photocurrent measurement system of OTE/H<sub>2</sub>DBuPP-n using I<sup>-</sup>/I<sub>3</sub><sup>-</sup> redox couple in the electrolyte system.<sup>18</sup> The photocurrent response recorded following the excitation of OTE electrode in the visible light region is shown in the insertion of Fig. 3B. The photocurrent response is prompt, steady and reproducible during repeated on/off cycles of the visible light illumination. Blank experiments conducted with OTE (i.e., by excluding H<sub>2</sub>DBuPP nanorod) produced no detectable photocurrent under the same

experimental conditions. The incident photon-to-photocurrent efficiency (IPCE) spectrum (spectrum *a* in Fig. 3B) also shows a broad photoresponse in the visible region (maximum IPCE: ~5.5% at 460 nm),<sup>19</sup> which parallels the corresponding absorption (spectrum *a* in Fig. 2A) and excitation spectra (spectrum *b* in Fig. 3B). These experiments confirmed the role of H<sub>2</sub>DBuPP nanorod towards harvesting light energy and generating photocurrent during the operation of a photoelectrochemical cell.<sup>20</sup>

In conclusion, we have succeeded in constructing supramolecular nanorods and fibers of 5,15-diaryl substituted porphyrins by sonication method. Utilizations of sonication and steric control of substituents are key factors for this unusual molecular aggregation phenomenon. The organized rod-shaped assembly also demonstrates efficient light-harvesting and photocurrent generation properties in the visible region. This simple and new method combined by design of molecular structure and sonication treatment could pave the way for developing light harvesting assemblies or optical and electronic devices.

This work was partially supported by Grant-in-Aids for Scientific Research (No. 19710119 to T.H.) and special coordination funds for promoting science and technology from the Ministry of Education, Culture, Sports, Science and Technology, Japan. We also thank Dr. T. Okubo (Kinki Univ.) and Dr. Y. Takamura (JAIST) for helpful discussion.

## Notes and references

1. G. M. Whitesides and B. Grzybowski, *Science*, 2002, **295**, 2418.
2. (a) H. Kasai, H. S. Nalwa, H. Oikawa, S. Okada, H. Matsuda, N. Minami, A. Kakuta, K. Ono, A. Mukoh and H. Nakanishi, *Jpn. J. Appl. Phys.*, 1992, **31**, L1132; (b) H. Masuhara, H. Nakanishi and K. Sasaki, *Single Organic Nanoparticles*; Springer: Heidelberg, 2003; (c) A. J. Gesquiere, T. Uwada, T. Asahi, H. Masuhara, and P. F. Barbara, *Nano Lett.*, 2005, **5**, 1321.
3. (a) D. Kim and A. Osuka, *J. Phys. Chem. A*, 2003, **107**, 8791; (b) M. U. Winters, E. Dahlstedt, H. E. Blades, C. J. Wilson, M. J. Frampton, H. L. Anderson and B. Albinsson, *J. Am. Chem. Soc.*, 2007, **129**, 4291; (c) J. N. H. Reek, A. E. Rowan, R. d. Gelder, P. T. Beurskens, M. J. Crossley, S. D. Feyter, F. d. Schryver and R. J. M. Nolte, *Angew. Chem. Int. Ed. Engl.*, 1997, **36**, 361; (d) M.-S. Choi, T. Aida, H. Luo, Y. Araki and O. Ito, *Angew. Chem., Int. Ed.*, 2003, **42**, 4060.
4. (a) T. Hasobe, P. V. Kamat, V. Troiani, N. Solladie, T. K. Ahn, S. K. Kim, D. Kim, A. Kongkanand, S. Kuwabata, and S. Fukuzumi, *J. Phys. Chem. B*, 2005, **109**, 19; (b) T. Hasobe, H. Imahori, P. V. Kamat, T. K. Ahn, S. K. Kim, D. Kim, A. Fujimoto, T. Hirakawa and S. Fukuzumi, *J. Am. Chem. Soc.*, 2005, **127**, 1216.
5. (a) N. Nagata, S.-i. Kugimiya, and Y. Kobuke, *Chem. Commun.*, 2000, 1389; (b) G. A. Mines, H.-C. Tzeng, K. J. Stevenson, J. Li and J. T. Hupp, *Angew. Chem., Int. Ed.*, 2002, **41**, 154; (c) P. A. J. de Witte, M. Castriciano, J. J. L. M. Cornelissen, L. M. Scolaro, R. J. M. Nolte and A. E. Rowan, *Chem. Eur. J.*, 2003, **9**, 1775; (d) B. L. Iverson, K. Shreder, V. Kral, P. Sansom, V. Lynch, and J. L. Sessler, *J. Am. Chem. Soc.*, 1996, **118**, 1608.
6. (a) Z. Wang, C. J. Medforth and J. A. Shelnutt, *J. Am. Chem. Soc.*, 2004, **126**, 15954; (b) Z. Wang, C. J. Medforth and J. A. Shelnutt, *J. Am. Chem. Soc.*, 2004, **126**, 16720; (c) A. D. Schwab, D. E. Smith, C. S. Rich, E. R. Young, W. F. Smith and J. C. dePaula, *J. Phys. Chem. B*, 2003, **107**, 11339; (d) A. D. Schwab, D. E. Smith, B. Bond-Watts, D. E. Johnston, J. Hone, A. T. Johnson, J. C. dePaula and W. F. Smith, *Nano Lett.*, 2004, **4**, 1261; (e) J. S. Hu, Y. G. Guo, H. P. Liang, L. J. Wan and L. Jiang, *J. Am. Chem. Soc.*, 2005, **127**, 17090; (f) R. Harada and T. Kojima, *Chem. Commun.*, 2005, 716; (g) T. Hasobe, S. Fukuzumi and P. V. Kamat, *J. Am. Chem. Soc.*, 2005, **127**, 11884; (h) Q. Zhou, C. M. Li, J. Li, X. Cui, and D. Gervasio, *J. Phys. Chem. C*, 2007, **111**, 11216; (i) V. Snitka, M. Rackaitis, and R. Rodaite, *Sensor. Actuat. B-Chem.*, 2005, **109**, 159; (j) H. Matsui and R. MacCuspie, *Nano Lett.*, 2001, **1**, 671; (k) B. Liu, D.-J. Qian, M. Chen, T. Wakayama, C. Nakamura, and J. Miyake, *Chem. Commun.*, 2006, 3175; (l) L.-L. Li, C.-J. Yang, W.-H. Chen, and K.-J. Lin, *Angew. Chem., Int. Ed.*, 2003, **42**, 1505.
7. (a) C. M. Drain, G. Smeureanu, S. Patel, X. Gong, J. Garnod and J. Arijeloyea, *New J. Chem.*, 2006, **30**, 1834; (b) T. Kishida, N. Fujita, K. Sada and S. Shinkai, *J. Am. Chem. Soc.*, 2005, **127**, 7298; (c) S. C. Doan, S. Shanmugham, D. E. Aston and J. L. McHale, *J. Am. Chem. Soc.*, 2005, **127**, 5885; (d) T. Hasobe, H. Imahori, S. Fukuzumi, and P. V. Kamat, *J. Mater. Chem.*, 2003, **13**, 2515; (e) R. Rotomskis, R. Augulis, V. Snitka, R. Valiokas, B. Liedberg, *J. Phys. Chem. B*, 2004, **108**, 2833; (f) S. Okada and H. Segawa, *J. Am. Chem. Soc.*, 2003, **125**, 2792.
8. (a) D. Horn and J. Rieger, *Angew. Chem., Int. Ed.*, 2001, **40**, 4330; (b) G. Ruecroft, D. Hipkiss, T. Ly, N. Maxted and P. W. Cains, *Org. Process Res. Dev.*, 2005, **9**, 923; (c) D. K. Bucar and L. R. MacGillivray, *J. Am. Chem. Soc.*, 2007, **129**, 32.
9. A. Osuka and H. Shimidzu, *Angew. Chem., Int. Ed.*, 1997, **36**, 135.
10. After sonication treatment, the initial solution dramatically changes to suspended condition to form assembled structures. See: Fig. S1.
11. We have also analyzed the structure of H<sub>2</sub>DBuPP nanorods prepared in sonicated suspension with different frequency (28 kHz). The length distribution is  $5.67 \pm 2.50 \mu\text{m}$ .
12. Sonication time-dependent formation of H<sub>2</sub>DBuPP assemblies were examined by TEM (Fig. S4). From 1 to 5 min after sonication, a dozen of small H<sub>2</sub>DBuPP nanoparticles were observed. From 5 to 20 min, formation and growth of rod-like structures were clearly observed. See: Fig. S4.
13. Self-assembled porphyrins can be reverted back to their monomeric form by diluting the solution with toluene, which was also confirmed by the absorption spectrum, NMR and MULDI/TOF MASS analyses (Fig. S6).
14. The crystal packing pattern of H<sub>2</sub>DPP (herringbone type) is totally different from that of H<sub>2</sub>TPP (head-to-tail type). In the case of H<sub>2</sub>DPP, the phenyl groups are presented outside of the herringbone structure, and porphyrin planes directly interact with respect to one another (smallest distance of two planes: 3.265 Å), whereas the phenyl groups interact with the its nearest neighbor porphyrin planes in H<sub>2</sub>TPP structure (distance: 3.616 Å). The difference also may have an influence on the self-assembled structures. See Fig. S7 and the following reference papers, H<sub>2</sub>DPP: A. D. Bond, N. Feeder, J. E. Redman, S. J. Teat, and J. K. M. Sanders, *Crystal Growth & Design*, 2002, **2**, 27, H<sub>2</sub>TPP: K. Kano, K. Fukuda, H. Wakami, R. Nishiyabu, and R. F. Pasternack, *J. Am. Chem. Soc.*, 2000, **122**, 7494.
15. We can see strong diffraction peaks of *a* and *c* axes such as (100) and (002) in the unit cell, whereas the diffraction intensity based on *b* axis is very weak (pattern *a* in Fig. S5A). Considering the unit cell structure (monoclinic structure: dihedral angles 90° in axes *a-b* and *b-c*), growth direction of the rod-crystals may be *b* axis direction (Fig. S7).
16. In the case of H<sub>2</sub>TBuPP assemblies, rectangular crystal growth was observed after 6 days of standing (Fig. S8).
17. Fluorescence lifetime of H<sub>2</sub>DBuPP nanorod film is strongly quenched as compared to the corresponding H<sub>2</sub>DBuPP drop-cast film and toluene solution. The lifetime of H<sub>2</sub>DBuPP nanorod film (421 ps: 94%) is much shorter than those of the drop-cast film (750 ps: 45% and 6023 ps: 55%) and in toluene solution (9700 ps: 100%). This shows additional deactivation pathways for the singlet excited state of H<sub>2</sub>DBuPP arising from the interaction between H<sub>2</sub>DBuPP and its nearest neighbor in the nanorod structures. See: Fig S9.
18. T. Hasobe, S. Fukuzumi, S. Hattori, and P. V. Kamat, *Chem. Asian J.*, 2007, **2**, 265.
19. The IPCE values were calculated by the following: IPCE (%) =  $100 \times 1240 \times I_{sc} / (I_{inc} \times \lambda)$ , where  $I_{sc}$  is the short circuit photocurrent (A/cm<sup>2</sup>),  $I_{inc}$  is the incident light intensity (W/cm<sup>2</sup>), and  $\lambda$  is the wavelength (nm).
20. We have also measured a photocurrent action spectrum of H<sub>2</sub>DBuPP drop-cast film. The action spectrum is in agreement with the corresponding absorption spectrum (spectrum *b* in Fig. 2b). See: Fig. S10.

---

## A graphical contents entry

